Research Square

Preprints are preliminary reports that have not undergone peer review.
They should not be considered conclusive, used to inform clinical practice,
or referenced by the media as validated information.

UWB fastly-tunable 0.5-50 GHz RF transmitter based on integrated photonics

Fabio Falconi
Sant'Anna School of Advanced Studies
Claudio Porzi
Sant'Anna School of Advanced Studies
Filippo Scotti
CNIT
Giovanni Serafino
Sant'Anna School of Advanced Studies
Antonio Malacarne
CNIT
Paolo Ghelfi
CNIT https://orcid.org/0000-0002-7762-7843
Antonella Bogoni (antonella.bogoni@cnit.it)
Sant'Anna School of Advanced Studies-CNIT https://orcid.org/0000-0002-8240-2171

Article

Keywords: Software-defined Ultra-wideband, Tunable Radio Frequency, Robot Localization Mapping, High Precision Radars, Photonic Chip, Microwave Photonics

Posted Date: June 29th, 2021

DOI: https://doi.org/10.21203/rs.3.rs-562494/v1

License: This work is licensed under a Creative Commons Attribution 4.0 International License.
Read Full License

Version of Record: A version of this preprint was published at Journal of Lightwave Technology on January 1st, 2021. See the published version at https://doi.org/10.1109/JLT.2021.3135861.

UWB fastly-tunable 0.5-50 GHz RF transmitter based on integrated photonics

Fabio Falconi[1], Claudio Porzi[1], Filippo Scotti[2], Giovanni Serafino[1], Antonio Malacarne[2], Paolo Ghelfi[2], & Antonella Bogoni[1,2]

[1] *TeCIP Institute, Scuola Superiore Sant'Anna, Via Moruzzi 1, 56124 Pisa, Italy*

[2] *National Laboratory of Photonic Networks, Inter-university National Consortium for Telecommunications (CNIT), Via Moruzzi 1, 56124 Pisa, Italy*

Antonella.bogoni@cnit.it

ABSTRACT:

In the last decade, the interest in software-defined ultra-wideband (UWB) and tunable radio frequency (RF) apparatuses with low size, weight, and power consumption (SWaP), has grown dramatically, pushed by the new 6G vision where, RF equipment shall enable a large number of fundamental applications as UWB communications, robot localization mapping and control and high precision radars, all of them contributing in revolutionizing our life style.

Unfortunately, the coexistence of ultra-wideband and software-defined operation, tunability and low SWaP represents a big issue in the current RF technologies.

In this article, to the best of our knowledge, the first example of a complete tunable software-defined RF transmitter with low footprint (i.e. on photonic chip) is presented exceeding the state-of-the-art for the extremely large tunability range of 0.5-50 GHz without any parallelization of narrower-band components and with fast tuning (<200μs). This first implementation, represents a breakthrough in microwave photonics.

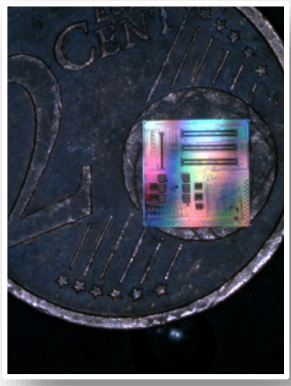

Fig. 1. The implemented silicon photonic chip including the 0.5-50GHz tunable RF transmitter

MAIN TEXT:

In the last decade, the interest in software-defined ultra-wideband (UWB) and tunable radio frequency (RF) apparatuses with low size, weight, and power consumption (SWaP), has grown dramatically, pushed by the new 6G vision where new human-centric services will be made possible by

combinations of connected smart devices, mobile robots, and avatars [1]. In this vision, RF equipment shall enable a large number of fundamental applications as UWB communications [2], robot localization mapping and control [3]-[6] and high precision radars [7]-[9], all of them contributing in revolutionizing our life style through breakthroughs in communications (e.g., intuitive ubiquitous connectivity), in medicine (e.g., wearable devices and tele-medicine) , in security (e.g., pervasive situational awareness), in work processes (e.g., Industry 4.0), etc.. Tunable UWB apparatuses, i.e., systems with a very large fractional bandwidth and an absolute bandwidth > 500 GHz, also providing a wide frequency tunability, exhibit a low and tunable power spectral density that allow them being used as overlay signals in the same frequency range as existing legacy services without causing undue interferences [10], therefore bypassing the increasing issues of the overcrowded RF spectrum and the scarseness of available band.

In wireless communications, various UWB transmitters operating in the unlicensed band between 3.1 GHz and 10.6 GHz have been presented due to their benefits in term of high data rate, robustness to propagation fading, interference rejection, and coexistence with narrow band systems [11],[12]. UWB and frequency-agile communications offer additional advantages such as the implementation of the cognitive radio paradigm allowing to transmit in the less-crowded frequency regions [13], the undercover operations and the resistance to jamming thanks to the low spectral density and a superior obstacle penetration when working with long wavelengths [2], [14]. Moreover, fast frequency agility reduces the network latency and contributes to new functionalities as the tracking of high-speed moving users.

In the so-called Industry 4.0, precise location-aware applications also exploit low spectral density UWB signals for RF identification (RFID) [15]. Moreover, applications involving the use of robots have extended broadly, including services requiring the simoultaneous operation of multiple robots, for which the precise localization & mapping and remote control can take advantage of rapidly tunable wideband RF connections [3]-[6] with bandwidth requirements in line with the 6G trends.

Moreover, such systems of robots are extending their applications from their traditional industry field to several other fields as military and medicine.

In advanced radars systems (as those foreseen in autonomous-driving vehicles), the broadband and fast frequency flexibility allows the implementation of a high-resolution and robust imaging, (including the case of moving targets) also integrating sensing and communication functionalities [16]. Moreover, UWB radar systems can detect the time-frequency signature of the targets by digitally generating a wide variety of waveforms in different frequency ranges, tailored to the target type of interest [17].

High dynamic range and wideband operation across the full 0-40 GHz range and beyond are also required in electronic warfare systems, where such a kind of transmitters can be used as jammers for UWB communication links and radars [18]. Currently, the jammers work in specific RF bands, especially in the range 1-6 GHz, 5-18GHz.

For all the applications mentioned above, an UWB transmitter is requested that must be able to provide fast frequency agility, and software-defined operation with the additional request of optimized SWaP for reducing the carbon footprint and fitting mobile platforms.

Unfortunately, the coexistence of ultra-wideband operation, reconfigurability (i.e. software defined approach), tunability and low SWaP represents a big issue in the current RF technologies. In fact, large frequency tunability collide with the need to reduce SWaP, due to intrinsic limitations in state-of-the-art electronic and microwave components (in particular, tunable RF filters, mixers and oscillators). Currently the coverage of the UWB spectral range of interest is obtained through several narrower-band systems in parallel, thus leading to high SWaP and strongly limiting the applicability of the tunable UWB software-defined paradigm. In particular, a RF tunable UWB transmitter can be obtained with conventional technologies, exploiting a voltage controlled oscillator (VCO) [19] combined width a wideband IQ mixer or a battery of narrow band IQ mixers [20],[21], controlled by electrical switches and driven by a digital direct sysntethizer (DDS). This solution is mainly limited

in terms of tunability time (>1ms) and range (< 40 GHz) [19]. Moreover, the IQ mixers suffer from low image rejection, (<25 dBm).

On the other hand, photonic techniques are increasingly being proposed for implementing RF systems targeting those desired features [22]-[33].

In the last few years, in fact, photonics has been demonstrating attractive features for microwave applications as extremely wide operating frequency range and instantaneous bandwidth [23]-[25], fast tunable filtering [26], tunable photonics-based microwave mixing with very high port-to-port isolation, and intrinsic immunity to electromagnetic interferences [27]. In [28], an UWB photonics-based transmitter for radio-over-fiber systems has been proposed, presenting an operating BW larger than 60 GHz, although using, to operate at different frequencies, a bulky electronic synthesizer impeding desired low SWaP solutions. In [29], a filter-free photonics-based transmitter is presented operating up to 26GHz, exploiting commercial off-the-shelf components.

Moreover, integrated photonics technologies are rapidly maturing, promising a breakthrough in RF systems through miniaturized, reconfigurable and, wideband microwave photonics systems [30]-[32]. So far, the most of the efforts have been focused on the optimization of the photonic integrated components for satisfying the RF system requirements, mainly based on the most mature platform of silicon photonics [24],[30],[33],[34].

In this paper, a prototype of an innovative widely tunable RF transmitter with unprecedented performance and enabled by integrated photonics is presented, implemented on chip with a CMOS-compatible Silicon-on-Insulator (SOI) technology as shown in Fig. 1, and demonstrating a working frequency range from 0.5 GHz to 50 GHz with fast tuning time <200 μs. This first implementation, although being a proof-of-concept with few limited performance, represents a breakthrough in microwave photonics, since it pioneers the concept of a complete UWB and tunable RF system on a photonic chip with the potential to significantly fully exceed the current state-of-the-art. At the same time, it also allows to experiencing the benefits and limitations of the silicon photonics platform for implementing complete microwave systems.

Fig. 2 (left) shows the architecture of the tunable photonics-based RF transmitter.

The generation of the tunable desired RF signal is based on the beating in a photodiode (PD) between an optical replica of the waveform to be transmitted, and a tunable optical carrier, producing at the output an RF signal holding the waveform to be transmitted, translated at a center frequency equal to the detuning between the two optical signals. In more detail, the waveform to be transmitted is digitally-generated thorugh a direct digital synthesizer (DDS) and converted in the analog domain at intermediate frequency (IF) f_{IF} by means of a digital-to-analog converter (DAC) (inset B). The optical replica of the waveform is obtained through the modulation of an input laser (inset A) in single-sideband carrier-suppression (SSB-CS) format, as shown in the lower arm of the scheme in Fig. 2. This modulation is obtained by means of a dual-parallel Mach-Zehnder modulator (MZM) driven by the I and Q components of the wavewform. This way, the obtained optical single-sideband signal (inset C) represents the optical replica of the original waveform.

On the other hand, a tunable optical carrier is obtained in the upper arm of the scheme of Fig. 2 by the tunable selection of one the optical lines out of an optical comb. The optical comb is generated by modulating the input laser by means of a phase modulator (PM) driven by an electrical fixed clock at frequency f_{clock} (inset E). This way, the comb line spacing is equal to f_{clock} (inset F). Then, a tunable optical filter selects one of the comb line (inset G) at the desired RF distance from the sideband (inset C). In particular, the selected line frequency is $f_{laser} \pm n f_{clock}$, where n is an integer number that can be chosen from 0 to the maximum usable line number within the comb, and its sign indicates the lines on the left or right of the input laser

The SSB-CS modulator and the tunable optical filter are the most critical components of the scheme which required a custom design. The former one shall select one line out of the full comb with an excellent rejection, while the later one shall provide excellent carrier and cancelled sideband suppression.

The selected comb line and the single sideband are finally coupled (inset D) and injected into a Germanium photodiode where they beat and generate an electrical replica of the waveform at the desired RF (inset H). This signal is then sent to an RF front-end before the transmission.

The proposed transmitter architecture allows for a continuous tunability: a discrete coarse tunability is due to the selection of the comb line, with a granularity corresponding to the clock frequency (line spacing), while the fine tunability for assuring a continuous tunability is due to the possibility to change the IF value up to the f_{clock}.

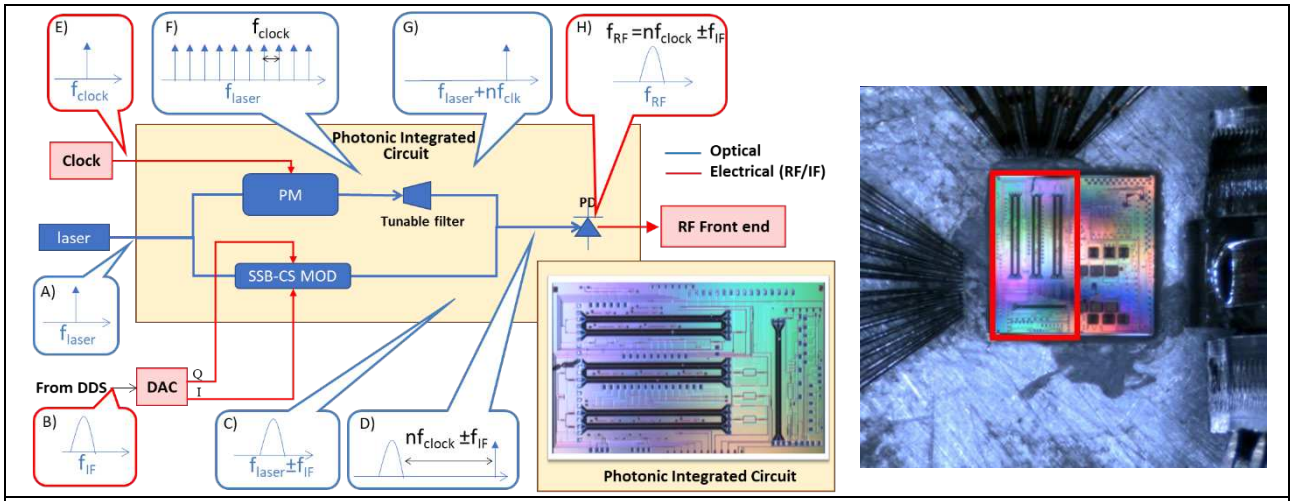

Fig. 2. (left): Architecture of the photonics-based RF transmitter and picture of the PIC. DAC: digital-to-analog converter; PM: phase modulator; SSB-CS MOD: single sideband-carrier suppression modulator; PD: photodiode; (right): Detail of the PIC under test showing the RF (top) and DC (left) probes and the optical fiber array (right). The tunable RF transmitter is contained in the region outlined in red

The photonic scheme (excluding the laser) has been implemented as a single photonic integrated circuit (PIC) exploiting the silicon-on-insulator (SOI) photonic platform at IMEC. Library blocks have been largely used (PM, PD, couplers/splitters), while the tunable filter and the architecture of the SSB-CS MOD have been suitably designed. The obtained chip dimension are 5x2.5mm^2. In the picture of the fabricated PIC in the insert of Fig. 2 (left) it is possible to recognize the three long MZM structures, one used for implementing the PM and two for implementing the SSB-CS MOD.

As first step, the single components of the implemented chip are characterized, thanks to monitoring points specifically inserted in the photonic circuit. Then, the test of the PIC as a whole system is

performed. For these tests, the PIC is placed on a thermo-electric cooler (TEC) that maintains its temperature with an accuracy of 0.01°C. The signal from the input laser and the monitoring output signals are injected and extracted from the PIC by means of an array of fibers, while the electrical IF/RF signals and control signals are injected or extracted from the chip through a multiprobe, as shown in Fig.2 (right).

The RF clock frequency has been set to 5GHz as best trade off between the expedience of using low f_{clock} values i.e. dense optical comb, for reducing the maximum required IF for continuous tunability, conseguently exploiting high performance narrow-band DAC, and the expedience of relaxing the optical filter requirement in terms of bandwidth i.e. corse optical comb lines. In fact, both wideband DDS and DAC (>5GHz) and narrow band optical filters (<5GHz) are critical component from a technological point of view. While 5GHz DDS and DAC are available on the market with performance suitable for UWB RF transmitters and optical filters with 3dB bandwidth of 5GHz have been demonstrated [26].

Table 1 reports the main measured parameters compared to the design specifications, for each single component, obtained during the chip characterization with a f_{clock}=5 GHz.

It is worth to note that the characterization does not highlight significant worsening, even better few specifications have been exceeded. As an example the targeted photondiode bandwidth was > 40GHz, but the measured values is >45 GHz and generation of carriers up to 50 GHz have been obtained.

In particular, details of the characterization of the two custom components (SSB-CS modulator and tunable optical filter) are reported.

Integrated component	Design specifications	Measured specifications
Grating coupler		
Loss	3,0dB	3,3dB
SSB-CS MOD		
Bandwidth	> 5GHz	> 15GHz
Min loss	< 7dB	< 8dB
V_π	< 9V	8V
Extinction ratio	> 25dB	40dB
PM		
Bandwidth	> 5GHz	> 15GHz
Loss	4dB	4,1dB
V_π	< 9V	8V
Tunable Filter		
3-dB bandwidth	< 5GHz	< 4GHz
35dB bandwidth	< 10GHz	< 10GHz
Stop-band	> 5THz	> 6THz
Tunability range	> 10 nm	> 10 nm
Tuning time	<200 μm	<200 μm
In-band loss	≤ 10dB	10 dB
Photodiode		
Bandwidth	≥40 GHz	>45 GHz (with bias=4V)

Table 1. Specifications of the single integrated photonics blocks of the photonics-based tunable RF transmitter

With reference to the inset of Fig. 3, the SSB-CS modulator is composed of two MZMs in parallel which operates in a carrier suppression configuration by means of an appropriate control of the thermal phase shifters on each MZM structure and of the tunable couplers which appropriately balance the phases and the amplitudes respectively so as to suppress the carrier. Furthermore, it is possible to obtain the single sideband configuration by driving the two MZMs with two signals out of phase by 90° (I and Q components) and balancing the phase and amplitude of the output signals of the Mach-Zehnder modulators through farther thermal phase shifters and tunable coupler. As a result, at the output of the SSB-CS modulator we will have a lateral band spaced from the wavelength of the original carrier by an amount equal to the frequency of the modulation signal (IF). The main quality parameter of an SSB-CS modulator is the suppression of the carrier and the unwanted sideband

compared to the main sideband. From Fig. 3 showing the measured optical spectra at the input (blue) and output (red) of the SSB-CS modulator, a suppression > 40 dB is obtained. This result is comparable to the values obtained with a discrete component of optical modulator in lithium niobate and exceed the performance of the IQ mixers that generate the single side band in conventional RF architectures with a suppression limited to 25 dB [20], [21].

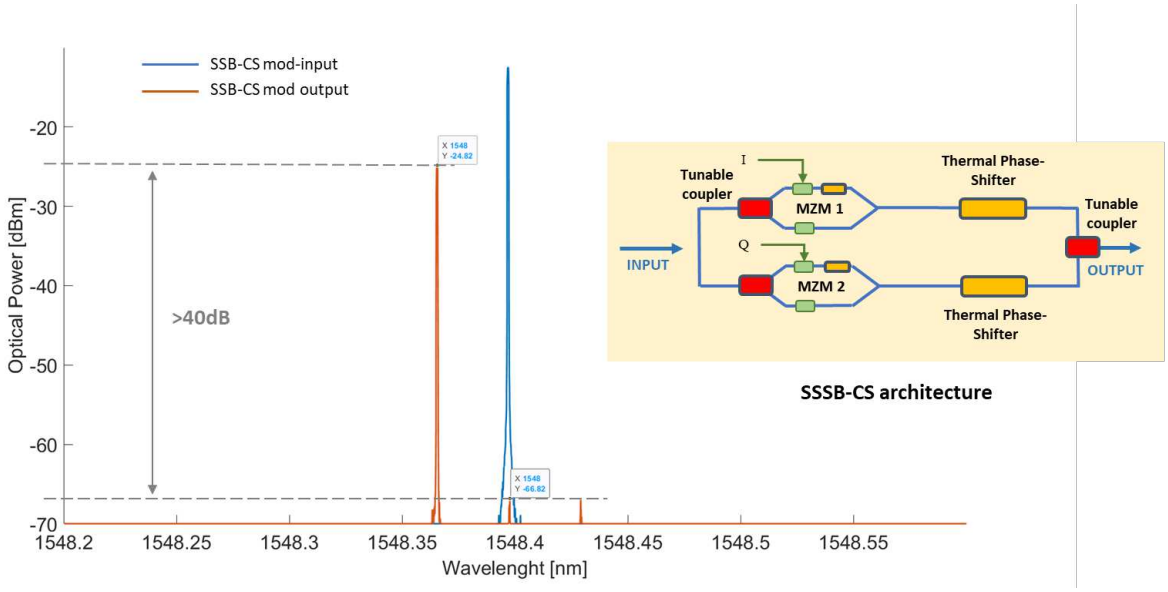

Fig. 3. Measured optical spectrum at the input (red curve) and at the output (blue curve) of the SSB-CS MOD. In the inset the SSB-MOD architecture is reported

The tunable optical filter has been realized as a cascade of phase-shifted Bragg gratings [26]. In particular as a 4th-order filter, in which five Bragg gratings are separated by four grating "defects" a quarter wavelength-long, where the phase is carefully controlled by means of micro-heaters above the defects themselves. Its 3dB bandwidth is as narrow as < 4GHz, while the 30dB bandwidth is < 10GHz (see Fig. 4-left) that is aligned with the state-of-the-art of optical filters. Consequently, the filter is able to select the desired line of the optical comb for f_{clock} (i.e. the comb frequency) ≥ 5GHz with an extinction ratio > 30dB.

The tunability range of the filter is also verified, showing almost constant performance across 10 nm (i.e., 1.25 THz) within the optical C band (1530-1565 nm), confirming that the optical filter is suitable for generating RF signals with carrier frequency ≥ 50 GHz.

The filter tunability speed determines the RF transmitter tunability speed. This parameter is measured by varying the control signal of one of the 4 micro-heaters (one for each filter stage) with a step function, so as to be able to move the filter from a condition of misalignment with the test signal, to a condition of perfect alignment (see Figure 4-right). By observing the time variation of optical power at the output of the filter, we have a precise measure of the tunability speed. The 10%-90% transient is less than 200 µs when the filter cools for shifting to higher frequencies, while it is faster (below 60 µs) when the filter is heated to shift it in the opposite spectral direction. This is because heating is applied by means of micro-resistors located exactly on top of the phase-shift defects in the Bragg gratings, so that an increase in the dissipated power in the micro-resistor affects the waveguide very quickly. Instead, cooling down the waveguide requires the excess heat accumulated within the PIC all around the heater to be dissipated in the chip, and hence to the TEC.

In both cases, the obtained filter tunability speed allows exceeding the transmitter tunability speed of conventional solutions limited to tunability time > 1ms.

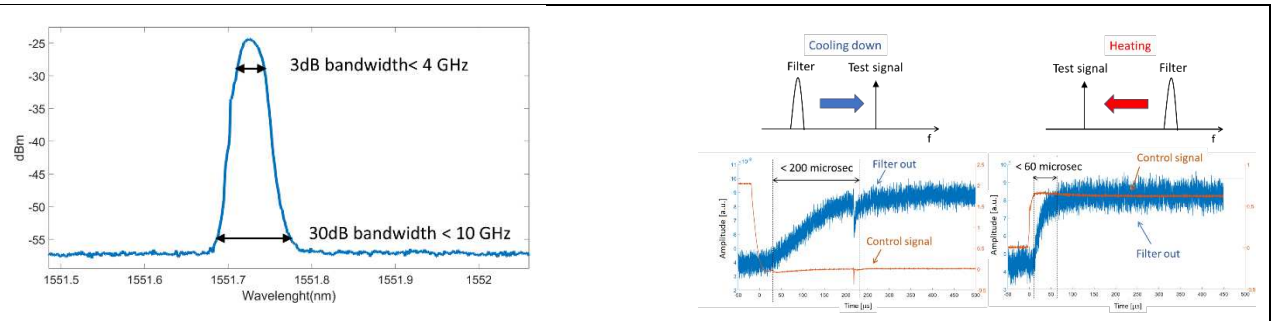

Fig. 4. (left): tunable optical filter transmission; (right) Time behavior of the signal at the output of the filter as it passes from a condition of misalignment with the signal to one of alignment, in the case of movement towards higher frequencies for cooling (left) and movement towards lower frequencies for heating (right).

After characterizing the single integrated components, the PIC is tested as a tunable UWB transmitter system, checking the tunability, and the signal purity in terms of phase noise and SFDR. Finally a communication experiments have been carry out in different RF bands.

Fig. 5 shows the results of the tunable generation of RF carriers across the C, X, Ku, K, and Ka bands, in the case of sinusoidal waveform at f_{IF} = 4 GHz (used as upper or lower SSB). The bandwidth of the electrical spectrum analyzer limited the visualization of the generated RF signals to 40GHz, but RF signals have been generated up to 50 GHz (V band) . In all cases, the spurious tones are suppressed > 25dB thanks to the excellent extinction ratio of both the filter and the SSB-CS modulator. However, it is worth to notice that the optical filter and the SSB-CS modulator, measured as stand-alone devices, both guarantee an extinction ratio > 30 dB. When tested as a system, the DC controls of the two devices turn out to induce mutual thermal crosstalk, which affects the optimization of their working point and results in a reduction of the spurious rejection. Thermal crosstalk reduction is possible digging trenches between the components, acting as thermal insulators.

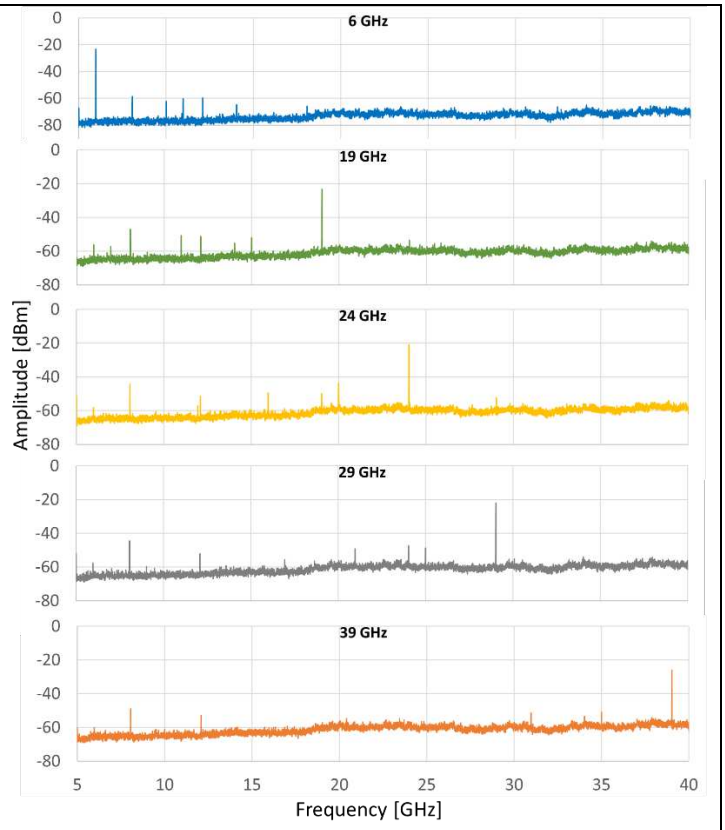

Fig. 5. RF carriers generated in C, X, Ku, K and Ka bands;

In order to study the quality of the generated tunable signals, the RF transmitter is characterized in terms of phase noise. Fig. 6(left) shows the phase noise power spectral density of the RF carrier generated at high frequencies (35, 40, 45, 50 GHz), where a higher noise level is expected (the noise power increase is theoretically proportional to the frequency multiplication factor square). The comparison with the reference clock signal at 5 GHz (in our case, a synthesizer) theoretically reported at the minimum analized frequency, i.e. 35 GHz (i.e. translated 17dB upwards), is also swown in order to facilitate the comparison. Phase noise curves are measured in a range 1 KHz - 40 MHz of frequency offset from the nominal carrier frequency. The range has been chosen according to the

requirements of communication application and considering the limit of the instrument at 40 MHz. The phase noise of the signal generated at 45 and 50 GHz is also reported, even though this frequency is outside the accepted range of the empolyed electrical spectrum analyser (Fig. 6 left).

The comparison of the phase noise curves presents at the extremes of the offset frequency, a gap in dBc/Hz aligned with the expected ideal gap due to the different tested carrier frequency (i.e. 20 dB ideal gap from 5GHz to 50 GHz), while in the central range (around 5 – 800 KHz), there is a residual discrepancy, with a wide peak centered at about 35 KHz. Such additional phase noise is introduced by the optical filter on the selected comb mode, due to the fluctuaction of the filter spectral response caused by the temperature control inaccuracy. Such fluctuation translates into phase noise of the generated RF tone after beating of the filtered optical mode with the sideband, at the PD. As a matter of fact, such additional spectral "bell" appears to be identical for each generated RF tone. Based on the reported phase noise curves, the temporal jitter of each generated RF tone is then calculated in the range 1 KHz – 40 MHz and reported by Fig. 6 (right), obtaining in all cases values lower than 170 fs, with a slight improvement for higher frequencies (from 169 fs at 35 GHz, down to 123 fs at 50 GHz) due to the constant contribution of temperature fluctuation, as stated before. The obtained jitter, although already comparable with the state-of-the-art of VCO (40 fs up to 32 GHz [19]), can be improved with a better temperature control.

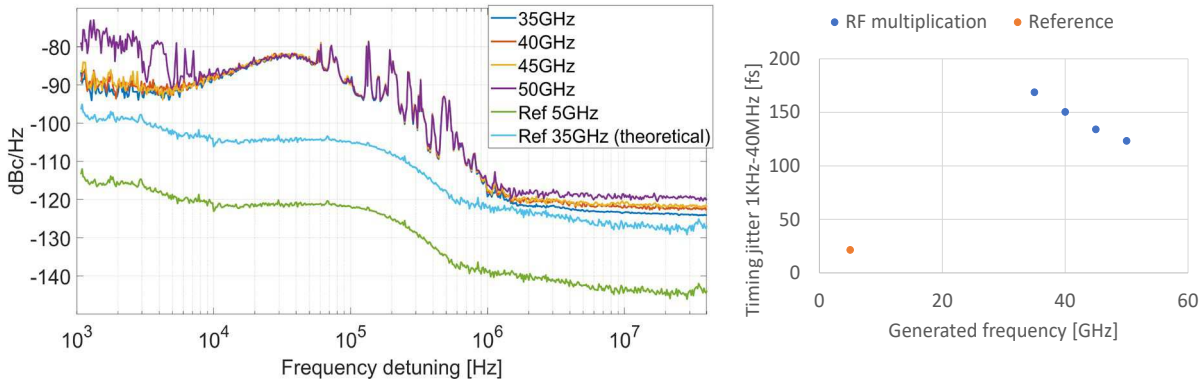

Fig. 6. (left) Phase noise curves of the RF signal generated for different values of the carrier. (right) Calculated timing jitter for each generated RF carrier.

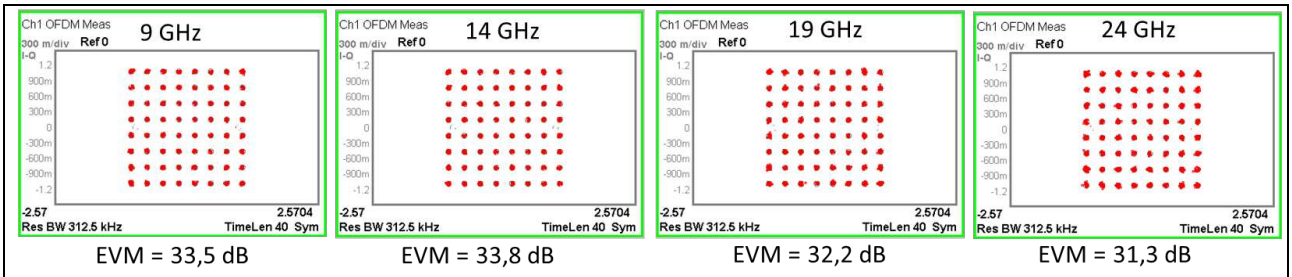

Fig. 7. 64QAM constellations generated at 9, 14, 19, 24 GHz (instrument limited to 26 GHz).

The software-defined photonics-based transmitter is also characterized in terms of its ability to generate a real communication signal, as shown in Figure 7. The maximum signal bandwidth is limited by the DAC bandwidth, in this case 5GHz. Here, the data signal is generated at an intermediate frequency of 4.063 GHz and modulated with 64QAM format. The clock signal is set again at 5 GHz. The up-converted version of the signal (at the carrier frequencies of 9, 14, 19, and 24 GHz), generated by the beating in the photodiode, is then analyzed using a vector signal analyzer. The performance is evaluated by measuring the error vector magnitude (EVM). Here the carrier frequency of the signal is limited by the bandwidth of the vector signal analyser, which is < 26 GHz. The EVM measurement detects variations < 3 dB as the frequency varies, and a penalty with respect to the reference signal (i.e. obtained without tunable up-conversion) of less than 4 dB in all cases.

Photonics-based tunable RF transmitter	RF State of the art (VCO + IQ mixer battery)	Measured specifications	Potential performance
Tunability range	≤ 40 GHz	0.5 GHz – 50 GHz	0.5 GHz – 100 GHz
Tunability speed	>1 ms	≤ 200µs	≤ 200 µs
SFDR	≥25 dB	≥25 dB	≥40 dB
Max instantaneous bandwidth	≤ 5 GHz Limited by the DAC	≤ 5GHz Limited by the DAC	≤5 GHz Limited by the DAC
Jitter [1kHz-10MHz]	<40 fs (up to 32 GHz)	<170 fs	<50 fs
Waveform	Software-defined	Software-defined	Software-defined
Conversion loss	≥ 10 dB	≈ 66 dB	≤ 10 dB

Table 2. Specifications of the photonics-based tunable RF transmitter

Table 2 (central column) summarizes all the obtained system performance and compares the obtained results with the RF state-of-the-art (left column) represented by the use of wideband VCO cascaded with a battery of narrower band IQ mixers. It is worth to note that the proposed photonics-based RF transmitter is a laboratory prototype, while the state-of-the-art comparison has been done with commercial components. In this sense the proposed technology has the potential to strongly improve its performance. For this reason, the achievable performance of the proposed solution after an optimization of the technological platform, as suggested by this proof-of-concept implementation, is also reported in the right column.

The implemented RF transmitter is able to generate tunable RF signals up to 50 GHz without any parallelization of narrower band components, and to provide fast frequency reconfigurability in less than 200 μs, enhancing the state-of-the-art tunability time (>1ms).

The SFDR in this specific implementation is limited to 25 dB, aligned with the RF state-of-the-art, due to thermal crosstalk between components as already discussed. However, after eliminating thermal cross-talk as explained in the following, RF transmitters with SFDR > 40 dB can be obtained. In fact, the SSB-MOD is already providing a suppression ratio > 40dB, while optical filters with out-of-band rejection > 40 dB at 5GHz from the central frequency have already been demonstrated (roll-off ≥10dB/GHz) [26],[34].

The maximum instantaneous bandwidth (B) is limited to 5GHz, by the exploited DAC as in the RF state-of-the-art. The limit imposed by the photonic subsystem is much higher. It comes from the photodiode bandwidth (<45GHz) that has to be > f_{RF}+B/2 in order to be able to generate the beating between the selected comb line and the optical sideband (i.e. the digitally generated waveform) with instantaneous bandwidth B at spectral distance f_{RF} from the laser. Integrated photodiodes have already been demonstrated to exceed a 100GHz bandwidth [35], allowing for a RF signal generation beyond 100GHz. The obtained jitter < 170fs is comparable with the state-of-the-art of electronic solutions limited to 40 GHz, but it is expected to be improved down to 50fs with a more accurate temperature

control of the optical filter as explained above. Moreover, the proposed solution guarantees software-defined waveforms as RF architectures.

The conversion loss of the implemented RF transmitter, defined as the ratio between the power of the IF input signal and the RF output signal, represents the main critical aspect of this implementation and also of all generic microwave photonics solutions: while RF technology provides values <10 dB, the state-of-the-art of microwave photonics systems based on silicon photonics presents a conversion loss ≤ 30 dB. In this implementation, the higher complexity of the architecture causes a measured conversion loss of 66 dB. However, this high value does not invalidate the demonstration of the potential of microwave photonics solutions for tunable UWB RF transceivers and it can be reduced as discussed in the following.

The relaxation of the footprint minimization (in this implementation is 5x2.5mm^2) could contribute to reduce the conversion loss, helping in reducing few technological impairments as the thermal crosstalk that prevent the simutaneous optimization of all components. In particular, the behavior of the different components of the circuit depends on their temperature which is controlled by means of suitable electrical signals. As already mentioned, the tunability of the circuit is obtained through a thermal control. Unfortunately, considering the small size of the chip, a thermal cross-talk phenomenon occurs, i.e. when the temperature of a component is changed, the temperature of the adjacent components changes too, thus affecting their operating point. This phenomenon induces a deviation of the working points of the components from the optimal conditions, introducing a penalty on the generated signal, especially in terms of conversion loss and spurious rejection. This criticality was highlighted during the characterization phase, generating a penalty of >5 dB on the spurious rejection in the generated RF signals. A possible solution to this problem is digging trenches between the components, acting as thermal insulators and thus allowing a reduction of the thermal crosstalk.

The conversion loss can also be improved reducing the losses in the photonic circuit and introducing optical amplification stages. Optical amplifiers can not be realized in silicon photonics , but their implementation requires a hybrid integration, i.e., a technology capable of putting together PICs

realized with different materials. Such approach would permit to integrate active components, i.e. optical amplifiers, on silicon platform. Another technological advance for reducing the conversion loss consists in reducing the Vπ, i.e., the voltage necessary for modulators to transfer intermediate frequency signals to the optical domain, and reduce their optical attenuation and nonlinearities. To date, the best technology for modulator implementation is the bulk lithium niobate (LN), a non-integrated technology that has dominated the telecom industry scene for decades, where the Pockels electro-optical effect warrants implementation of low attenuation and highly linear modulators. Recently, integrated lithium niobate on insulator (LNOI) technology has been developed, which enables on-chip LN modulators with very low Vπ and with dimensions typical of photonic chips [36]-[38]. All the above considerations allow to estimate a possible improved conversion loss ≤ 10 dB, aligned with the RF state-of-the-art, if an hybrid photonic integration approach is exploited for integrating active components with LNOI modulators.

Conclusions

A breakthrough implementation of a 0.5-50 GHz tunable RF transmitter based on integrated photonics has been presented. It has been obtained through a tunable up conversion in the optical domain of a digitally generated waveform at intermediate frequency, completely avoiding the parallelization of components with limited bandwidth. The chip characterization confirms the potential of microwave photonics for overcoming the current challenges of RF systems in terms of fast frequency agility and broadband coverage, maintaining a low SwAP and meeting the RF transmitter future requirements in the field of communications and sensing for a large range of applications. Moreover, this first implementation brought out the main technological issues of silicon photonics that will drive further developments of hybrid integrated photonics platforms. In a dual way, the same microwave photonic solution can allow to implement in the optical domain a down conversion of a received RF signal to intermediate frequency, resulting in an ultra wideband tunable RF receveir [39].

In this sense the reported demonstration represents a fundamental step toward the implementation of a building block for next generation flexible and ultrawideband transceivers to be exploited in several emerging markets.

ACKNOWLEDGEMENTS:

This work has been supported by the Italian Defence, within the project DISTURB

REFERENCES:

[1] M. Maier, A. Ebrahimzadeh, “Toward 6G: A New Era of Convergence”, IEEE Press Wiley, January 2021, ISBN: 978-1-119-65802-3
[2] White Paper, “Cisco Visual Networking Index: Global Mobile Data Traffic Forecast Update 2017–2022” (2019).
[3] L. Han, B. Dzodzo, H. Qian, Y. Xu, “The State of the Art in Mapping and Navigation for Household Service”, Household Service Robotics, Accademic Press, 2015
[4] S. Saeedi, Michael Trentini, Mae Seto, Howard Li , “Multiple-Robot Simultaneous Localization and Mapping: A Review” Journal of Field Robotics, Vol. 33, n.1, Pages 3-46 January 2016
[5] X. Zhu, J. Yi, J. Cheng and L. He, "Adapted Error Map Based Mobile Robot UWB Indoor Positioning," in IEEE Transactions on Instrumentation and Measurement, vol. 69, no. 9, pp. 6336-6350, Sept. 2020. doi: 10.1109/TIM.2020.2967114
[6] F. J. Perez-Grau, F. Caballero, L. Merino and A. Viguria, "Multi-modal mapping and localization of unmanned aerial robots based on ultra-wideband and RGB-D sensing," *2017 IEEE/RSJ International Conference on Intelligent Robots and Systems (IROS)*, Vancouver, BC, Canada, 2017, pp. 3495-3502. doi: 10.1109/IROS.2017.8206191
[7] J.-Y. Park, Y. Lee, Y.-W. Choi, R. Heo, H.-K. Park, S.-H. Cho, S. H. Cho & Y.-H. Lim “Preclinical evaluation of a noncontact simultaneous monitoring method for respiration and carotid pulsation using impulse-radio ultra-wideband radar”, Scientific Reports NatureResearch, August 2019, https://doi.org/10.1038/s41598-019-48386-9
[8] D. B. Issa, M. Hajri, A. Kachouri, M. Samet & H. Samet “Reconfigurable UWB Transceiver for Biomedical Sensor Application”, Springer, BioNanoScience Vol. 7, pages 11–25, 2017
[9] J. W. Choi, D. H. Yim, and S. H. Cho “People Counting Based on an IR-UWB Radar Sensor”, IEEE Sensors Journal, Vol. 17, n. 17, September, 2017
[10] A. F. Molisch, “Ultra-wideband communications : An overview”, URSI Radio Science Bulletin, Vol. 2009, n. 329, June 2009
[11] M. Z. Win, et al., “History and Applications of UWB”, Proceedings of the IEEE, Vol. 97, No. 2, February 2009.
[12] G. Lee; J. Park; J. Jang; T. Jung; T. W. Kim “An IR-UWB CMOS Transceiver for High-Data-Rate, Low-Power, and Short-Range Communication”, IEEE Journal of Solid-State Circuits Vol. 54, n. 8, Aug. 2019
[13] W. S. H. M. W. Ahmad, N. A. M. Radzi, F. S. Samidi, A. Ismail, F. Abdullah, M. Z. JAamaludin and M. N. Zakaria, “5G Technology: Towards Dynamic SpectrumSharing Using Cognitive Radio Networks” IEEE Access, January 2020
[14] X. Liang, J. Deng, H. Zhang, et al. Ultra-Wideband Impulse Radar Through-Wall Detection of Vital Signs. Sci Rep 8, 13367 (2018). https://doi.org/10.1038/s41598-018-31669-y
[15] Y. Zhou, C. L. Law and J. Xia, "Ultra low-power UWB-RFID system for precise location-aware applications," 2012 IEEE Wireless Communications and Networking Conference Workshops (WCNCW), Paris, France, 2012, pp. 154-158, doi: 10.1109/WCNCW.2012.6215480.

[16] D. Ma, N. Shlezinger, T. Huang, Y. Liu, Y. C. Eldar. "Joint Radar-Communication Strategies for Autonomous Vehicles: Combining Two Key Automotive Technologies", IEEE Signal Processing Magazine Vol. 37, n. 4, July 2020
[17] J. D. Taylor, "Advanced Ultrawideband Radar: Signals, Targets, and Applications", CRC Press, December 14, 2016.
[18] M. Frater and M. J. Ryan "Electronic Warfare for the Digitized Battlefield", Artech House, January 2001.
[19] https://www.analog.com/en/products/adf4371.html#
[20] https://www.av-iq.com/avcat/ctl1642/index.cfm?manufacturer=analog-devices&product=hmc8038
[21] https://www.qorvo.com/products/frequency-converters/mixers
[22] P. Ghelfi, F. Laghezza , A. Bogoni, "Photonics for Radar Networks and Electronic Warfare Systems" Editors: IET SciTech Book Series: Radar, Antennas and Electromagnetics, 2019, ISBN: 9781785613760
[23] H. G. de Chatellus, L. R. Cortés, C. Schnébelin, M. Burla & J. Azaña "Reconfigurable photonic generation of broadband chirped waveforms using a single CW laser and low-frequency electronics", Nature Communications Vol. 9, n. 2438 2018
[24] J. Tang, B. Zhu, W. Zhang, M. Li, S. Pan & J. Yao "Hybrid Fourier-domain mode-locked laser for ultra-wideband linearly chirped microwave waveform generation", Nature Communications Vol. 11, n. 3814, 2020
[25] E. Ruggeri, A. Tsakyridis, C. Vagionas, G. Kalfas, R. M. Oldenbeuving, P. W. L. Van Dijk, C. G.H. Roeloffzen, Y. Leiba, N. Pleros, and A. Miliou "A 5G Fiber Wireless 4Gb/s WDM Fronthaul for Flexible 360° Coverage in V-Band massive MIMO Small Cells" IEEE Journal of Lightwave Technology, Vol 39, n.4, 2021
[26] C. Porzi, G. J. Sharp, M. Sorel and A. Bogoni, "Silicon Photonics High-Order Distributed Feedback Resonators Filters," in IEEE Journal of Quantum Electronics, vol. 56, no. 1, pp. 1-9, Feb. 2020,
[27] P. Ghelfi, F. Laghezza, F. Scotti, G. Serafino, A. Capria, S. Pinna, D. Onori, C. Porzi, M. Scaffardi, A. Malacarne, V. Vercesi, E. Lazzeri, F. Berizzi, and A. Bogoni, "A fully photonics-based coherent radar system", Nature, Vol. 507, pp. 341–345, 20 March 2014.
[28] O Omomukuyo, et al., "Performance Evaluation of a 60-ghz Multi-band Ofdm (mb-ofdm) Ultra-wideband Radio-over-fibre System", IEEE Journal on Selected Areas in Communications, 2011.
[29] D. Onori et al., "A Software-defined and Filter-free 0 26.5 GHz Ultra wideband RF Transmitter Enabled by Photonics", EuRAD 2017
[30] D. Marpaung, J. Yao & J. Capmany "Integrated microwave photonics" Nature Photonics vol. 13, pages 80–90, 2019
[31] F. Falconi, S. Melo, F. Scotti, M.N. Malik, M. Scaffardi, C. Porzi, L. Ansalone, P. Ghelfi, A. Bogoni, "A Combined Radar & Lidar System based on Integrated Photonics in Silicon-on-Insulator", IEEE Journal of Lightwave Technology, Vol 39, n.1, 2021
[32] https://arxiv.org/abs/1905.12802
[33] R. Maram, S. Kaushal, J. Azaña, and L.R Chen "Recent Trends and Advances of Silicon-Based Integrated Microwave Photonics", Photonics vol. 6, n. 1, 2019.
[34] P. Dong et al., "GHz-bandwidth optical filters based on high-order sili-conringresonators,"Opt. Express, vol. 18, pp. 23784–23789, Nov. 2010
[35] S. Lischke, A. Peczek, F. Korndörfer, C. Mai, H. Haisch, M. Koenigsmann, M. Rudisile, D. Steckler, F. Goetz, M. Fraschke, et al. S. M "Ge Photodiode with -3 dB OE Bandwidth of 110 GHz for PIC and ePIC Platforms", 2020 IEEE International Electron Devices Meeting (IEDM), 10.1109/IEDM13553.2020.9372033
[36] M. Loncar et al., "An Integrated Low-Voltage Broadband Lithium Niobate Phase Modulator" IEEE Photonics Technology Letters vol. 31, n. 11, 2019
[37] M. Xu, et al. High-performance coherent optical modulators based on thin-film lithium niobate platform. Nat Commun vol. n. 11, 2020.
[38] P. Kharel, C. Reimer, K. Luke, L. He, and M. Zhang "Breaking voltage–bandwidth limits in integrated lithium niobate modulators using micro-structured electrodes", Optica, Vol. 8, n. 3, pp. 357-363, 2021, https://doi.org/10.1364/OPTICA.416155
[39] Onori D., Scotti F., Laghezza F., Bartocci M., Zaccaron A., Tafuto A., Albertoni A., Bogoni A., Ghelfi P. "A Photonically-enabled Compact 0.5 - 28.5 GHz RF Scanning Receiver", IEEE Journal of Lightwave Technology, Vol. 36, n. 10, pp. 1831-1839, 2018